

Proceeding Paper

Exploring BINOL-O-BODIPY-Based Dimers as Advanced Chromophoric Platforms Enabling Triplet State Population †

 Sergio Serrano-Buitrago ¹, Josué Jiménez ¹, Ruth Prieto-Montero ² , Florencio Moreno ¹ ,
Virginia Martínez-Martínez ² , Beatriz L. Maroto ¹  and Santiago de la Moya ^{1,*} 
¹ Departamento de Química Orgánica, Facultad de Ciencias Químicas, Universidad Complutense de Madrid, Ciudad Universitaria s/n, 28040 Madrid, Spain

² Departamento de Química Física, Facultad de Ciencia y Tecnología, Universidad del País Vasco-EHU, 48080 Bilbao, Spain

* Correspondence: santmoya@ucm.es; Tel.: +34-913945090

† Presented at the 26th International Electronic Conference on Synthetic Organic Chemistry, 15–30 November 2022; Available online: <https://sciforum.net/event/ecsoc-26>.

Abstract: An example of a new BODIPY design with triplet state population is reported: BINOL-O-BODIPY-based dimer. This new design combines two easily accessible structural features with a demonstrated capability of populating triplet states without the need for iodine or heavy metals: *meso-p*-phenylene-bridged BODIPY dimer and BINOL-O-BODIPY.

Keywords: BODIPY; triplet state; photosensitizer; fluorescence; singlet oxygen



Citation: Serrano-Buitrago, S.; Jiménez, J.; Prieto-Montero, R.; Moreno, F.; Martínez-Martínez, V.; Maroto, B.L.; de la Moya, S. Exploring BINOL-O-BODIPY-Based Dimers as Advanced Chromophoric Platforms Enabling Triplet State Population. *Chem. Proc.* **2022**, *12*, 15. <https://doi.org/10.3390/ecsoc-26-13671>

Academic Editor: Julio A. Seijas

Published: 17 November 2022

Publisher's Note: MDPI stays neutral with regard to jurisdictional claims in published maps and institutional affiliations.



Copyright: © 2022 by the authors. Licensee MDPI, Basel, Switzerland. This article is an open access article distributed under the terms and conditions of the Creative Commons Attribution (CC BY) license (<https://creativecommons.org/licenses/by/4.0/>).

1. Introduction

Chromophoric systems capable of populating triplet states (TSs) upon light absorption, i.e., triplet state photosensitizers (TS-PSs), have found widespread use in interesting applications, such as photodynamic therapy (PDT), luminescent oxygen sensing, photoinduced catalytic hydrogen photoproduction (i.e., photocatalytic water splitting), and photoredox organic reactions, among others [1–5]. The population of the TS is usually achieved after photoexcitation of the chromophore to the singlet state, followed by an intersystem crossing (ISC) between this state and an excited TS, T_n , of suitable energy [1,3].

Among all chromophoric systems, the BODIPY (boron dipyrromethene, e.g., **1** in Figure 1) family has emerged as one of the most interesting scaffolds for the development of TS-PSs due to their high light-absorption capacity and their wide chemical versatility that allows fine-tuning of key properties for the required ISC [6–9]. The main strategy employed to populate TSs in BODIPYs is the attachment of heavy atoms to the chromophore (e.g., iodine or transition metals; c.f. **1** and **2** in Figure 1; singlet oxygen quantum yield, ϕ_Δ , 0% vs. 83%). However, the ISC in these systems is so effective that it entails a virtual quenching of the BODIPY's fluorescence. The T_1 to S_0 ISC is so fast that the TSs usually show short lives, which are disadvantages for some applications (e.g., singlet oxygen-based PDT or phototheragnosis, that is, therapy using PDT and diagnosis by fluorescence from a single chemical agent). Moreover, the presence of these atoms can limit the use of the dye in biomedical-related applications, as PDT or phototheragnosis are, owing to their inherent toxicity [10,11].

Recently, other strategies have started being developed that avoid the use of heavy atoms, having the advantage of the possibility of balancing fluorescence and TS population. One of these strategies is the construction of *orthogonal BODIPY dimers*, in which the BODIPY chromophores are directly bonded, a process first reported by Akkaya and col. (**3** in Figure 1, with ϕ_{fl} (CHCl_3) 31% and ϕ_Δ (DCM) 46%) [12], although the synthesis of these dimers is usually tedious. Related to this, in 2017, Shao, Huang, and Dong [13], and Wu, Song, and Kuang [14] separately reported a dimer with two identical BODIPY units

linked through their *meso*-position via a *p*-phenylene bridge (**4** in Figure 1), whose synthesis is easier than that of the orthogonal dimers. This dimer also showed PS-TS capability, although significantly lower than the previous orthogonal one (ϕ_{fl} (DCM) 44% and ϕ_{Δ} (DCM) 7%) [13,14].

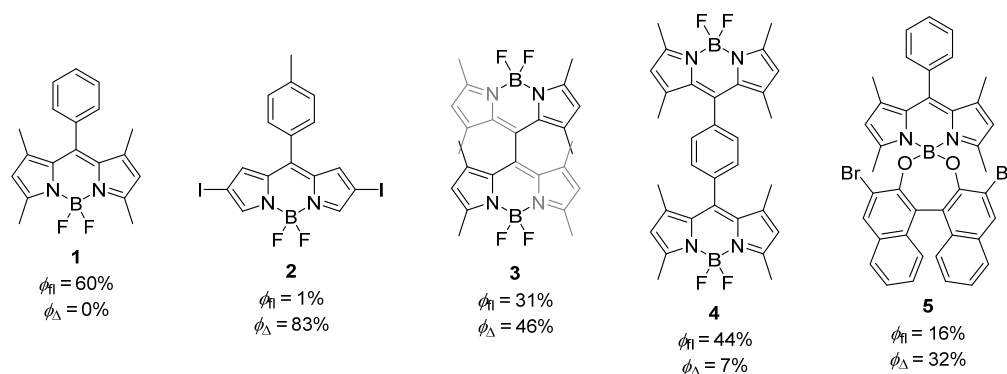


Figure 1. Selected examples of TS-PSs based on BODIPY dyes. (ϕ_{fl} : fluorescence quantum yield; ϕ_{Δ} : singlet oxygen quantum yield. Data in CHCl_3 or DCM solution, see text).

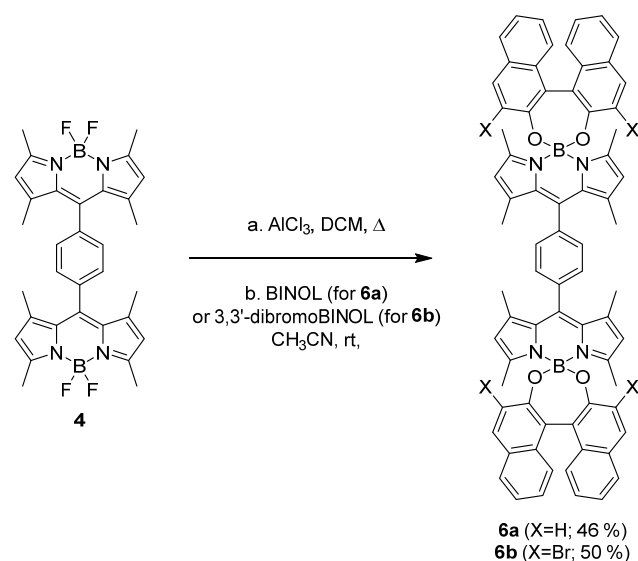
Another strategy is the one developed by de la Moya, Bañuelos, and Martínez-Martínez in BINOL-*O*-BODIPYs, based on the idea that intramolecular charge transfer (ICT) states can act as a pathway toward the ISC that leads to the TS. The authors demonstrated that it is possible to modulate the TS population, and consequently the singlet oxygen generation, by modulating the ICT, which in turn can be done by adjusting the electronic effects on both the BODIPY and the BINOL subunits [15–17]. For example, **5** (Figure 1), a BINOL-*O*-BODIPY based on **1** with demonstrated ICT state population, shows both fluorescence and singlet oxygen generation with a ϕ_{Δ} as high as 0.32 in CHCl_3 [16].

From these precedents, we hypothesized that the combination of these two designs (*meso-p*-phenylene-bridged BODIPY dimer and BINOL-*O*-BODIPY) could generate a synergy that would enhance the population of TSs, providing a new strategy for the development of advanced BODIPY-based TS-PSs. This communication shows preliminary results related to this investigation concerning the design, synthesis, and photophysical characterization, including fluorescence and singlet oxygen generation, of novel dyes combining both features.

2. Results and Discussion

For this preliminary study, we selected the *O*-BODIPY dimers, **6** shown in Scheme 1, involving BODIPY chromophores linked by their *meso* positions through a *p*-phenylene bridge and having two equal BINOL moieties, each one attached to the boron atom of each BODIPY subunit. We selected these dimers for their easy synthetic access and to be able to compare their performance to that exhibited by the corresponding *F*-BODIPY dimer precursor (**4**). As the BINOL unit, we chose BINOL and 3,3'-dibromobINOL for their demonstrated different capability of inducing ICT in BINOL-*O*-BODIPYs [15–17].

The synthesis of compounds **6** was carried out following the methodology developed by us for the synthesis of BINOL-*O*-BODIPYs from corresponding *F*-BODIPYs, based on the substitution of the fluorine atoms by the oxygens of the BINOL moiety (BINOL for **6a**; 3,3'-dibromobINOL for **6b**) activated by a Lewis acid, in this case, AlCl_3 [15]. The two compounds were successfully obtained in 46 and 50% yields, respectively, from parent *F*-BODIPY dimer **4** [13,14] (Scheme 1).



Scheme 1. Synthesis of BINOL-*O*-BODIPY dimers **6** from parent *F*-BODIPY **4**.

The selected set of *meso-p*-phenylene-bridged BODIPY dimers (**4**, **6a**, and **6b**) was photophysically and photochemically (singlet oxygen generation) characterized in a diluted chloroform solution. The obtained data are summarized in Table 1 and the absorption and fluorescence spectra are shown in Figure 2.

Table 1. Photophysical and photochemical ($^1\text{O}_2$ production) properties of *meso-p*-phenylene-bridged BODIPY dimers **4**, **6a**, and **6b** in diluted chloroform solution (3×10^{-6} M): absorption wavelength (λ_{ab}), molar absorption (ϵ_{max}), fluorescence wavelength (λ_{fl}), fluorescence quantum yield (ϕ_{fl}), fluorescence lifetime (τ) and $^1\text{O}_2$ quantum yield (ϕ_{Δ}).

| Compound | λ_{ab} (nm) | ϵ_{max} ($10^4 \text{ M}^{-1} \text{ cm}^{-1}$) | λ_{fl} (nm) | ϕ_{fl} | τ (ns) | ϕ_{Δ} |
|-----------|-------------------------------|--|-------------------------------|--------------------|-------------------------|-----------------|
| 4 | 502.0 | 5.9 | 522.0 | 0.39 | 3.86 | 0.05 |
| 6a | 518.0 | 8.7 | 530.0 | 0.00 | - | 0.03 |
| 6b | 507.0 | 5.1 | 530.5 | 0.06 | 0.73 (99%) 2.37 (1%) | 0.18 |

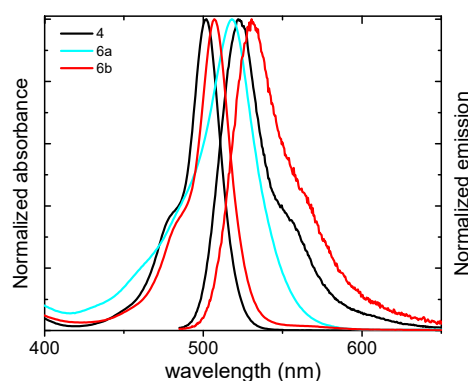


Figure 2. Height-normalized absorption and emission spectra of *meso-p*-phenylene-bridged BODIPY dimers **4**, **6a**, and **6b** in chloroform (3×10^{-6} M).

The *F*-BODIPY dimer **4** showed a moderate fluorescence quantum yield in chloroform ($\phi_{\text{fl}} = 0.39$, Table 1). The fluorescence was slightly more intense in more apolar solvents ($\phi_{\text{fl}} = 0.50$ in toluene [18]), but it drastically dropped as the polarity of the solvent increased ($\phi_{\text{fl}} = 0.01$ in acetone or acetonitrile, data not shown). This polarity effect is a characteristic

feature of the formation of a non-radiative ICT state, likely between the phenylene moiety and the BODIPY subunits. This dimer also showed, as it had been reported before [13,14], singlet oxygen photoproduction, although with a discreet yield ($\phi_{\Delta} = 0.05$ in chloroform), despite not having any iodine or heavy metal attached to the acting BODIPY chromophores. This fact could be explained by the ICT state acting as a pathway for the ISC toward the TS.

When introducing BINOL units at the borons to obtain **6**, the photophysical behavior changed, as it was expected [16]. Thus, BINOL-*O*-BODIPY dimer **6a**, with unsubstituted BINOL, demonstrated poorer photophysical behavior in terms of both fluorescence and singlet oxygen photoproduction than *F*-BODIPY dimer **4**. This effect could be explained by the electron donor ability of the BINOL moieties when compared to fluorine, which would activate a photoinduced electron transfer (PET) from a specific BINOL moiety to the corresponding BODIPY subunit, hampering both fluorescence and singlet oxygen capabilities of the dye in any solvent (analyzed from *c*-hexane to acetonitrile), similarly to the previously observed behavior of the analogous monomeric BINOL-*O*-BODIPY [16]. On the contrary, in the case of **6b**, a significant enhancement of the singlet oxygen production to nearly 20% (Table 1) was observed while keeping a modest fluorescence efficiency ($\phi_{fl} = 0.06$). In this case, the incorporation of electron-withdrawing bromine atoms into the BINOL unit decreased the electron donor ability of the BINOL moiety, avoiding the PET but still enabling the formation of the ICT state and leading to a significant TS population and, consequently, singlet oxygen photoproduction. Therefore, it was possible to modulate the TS population through the modulation of the probability of the ICT by choosing the right substitution in the BINOL moieties (hydrogen or bromine) in *meso-p*-phenylene-bridged BINOL-*O*-BODIPY dimers. These results are in line with the reported modulation in monomeric BINOL-*O*-BODIPYs [16]. However, the effect of introducing 3,3'-dibromobINOL moieties in the dimers (c.f. **6b** with **4** in Table 1) does not seem to be as effective as it was in the case of the monomeric BINOL-*O*-BODIPYs (for example, c.f. **5** with **1** in Figure 1).

3. Conclusions

We have reported a preliminary study on the development of a new, easily accessible design for the population of TSs in iodine-/heavy-metal-free BODIPYs. The new design combines two previous ones that proved successful for the population of TSs: *meso-p*-phenylene-bridged BODIPY dimer and BINOL-*O*-BODIPY with modulable ICT. Therefore, we built two BODIPY dimers in which the two BODIPY chromophores were linked through a *p*-phenylene bridge, and the involved boron atoms carried equal BINOL or 3,3'-dibromobINOL units. It was demonstrated that the transformation of an *F*-BODIPY dimer in the corresponding BINOL-*O*-BODIPY dimer could indeed increase the singlet oxygen photoproduction, although the observed increase was not as high as it had been for the transformation of a related monomeric *F*-BODIPY in the corresponding monomeric BINOL-*O*-BODIPY. Moreover, the population of TSs can be modulated, as it was the monomeric case, by carefully choosing the substituents in the BINOL moiety. This has been shown in the two examples selected for this preliminary communication: 3,3'-dibromobINOL-derived dimer **6b** can induce ICT and, therefore, the population of TS while keeping fluorescence, whereas unsubstituted-BINOL-derived dimer **6a** experiences a PET process that quenches fluorescence and avoids ICT-state and TS population. Further studies with a battery of unprecedented BINOL-*O*-BODIPY dimers, including those based on orthogonal BODIPY dimers or on other BINOL derivatives, are in progress to demonstrate these preliminary findings and set the bases for the development of easily accessible and heavy-atom-free PS-TSs on the basis of using ICT-modulable BINOL-*O*-BODIPY subunits.

4. Materials and Methods

4.1. Synthesis

General: Common solvents were dried and distilled by standard procedures. All starting materials and reagents were obtained commercially and used without further purification. Elution flash chromatography was conducted on silica gel (230 to 400 mesh

ASTM). Thin layer chromatography (TLC) was performed on silica gel plates (silica gel 60 F254, supported on aluminum). The NMR spectra were recorded at 20 °C, and the residual solvent peaks were used as internal standards. The NMR signals are given in ppm. The DEPT-135 NMR experiments were used for the assignment of the type of carbon nucleus (C, CH, CH₂, and CH₃). The FTIR spectra were recorded from neat samples using the ATR technique, and IR bands are given in cm⁻¹.

Synthesis of 6: Over a solution of **4** (50 mg, 0.088 mmol) in anhydrous dichloromethane (5 mL) under an argon atmosphere, AlCl₃ (61 mg, 0.44 mmol) was added, and the mixture refluxed for 3 h. After this time, the mixture was cooled down to room temperature, and then a solution of BINOL (1,1'-binaphth-2-ol, 126 mg, 0.44 mmol, for the synthesis of **6a**) or 3,3'-dibromoBINOL (3,3'-dibromo-1,1'-binaphth-2-ol, 195 mg, 0.44 mmol, for the synthesis of **6b**) in anhydrous acetonitrile (1 mL), was added and allowed to react for 24 h. Then, the reaction mixture was washed with water (3 × 20 mL), and the organic phase was dried over Na₂SO₄ and filtered. The solvent was evaporated under reduced pressure. The crude was purified by column chromatography on silica gel using hexane/CH₂Cl₂ 7:3 as the eluent.

6a: 43 mg (46%). Orange solid. *R*_f = 0.90 (CH₂Cl₂). ¹H NMR (CDCl₃, 300 MHz) δ 7.85 (d, *J* = 8.0 Hz, 4H), 7.79 (d, *J* = 8.8 Hz, 4H), 7.65 (s, 4H), 7.33 (ddd, *J* = 8.0, 6.6, 1.3 Hz, 4H), 7.26 (d, *J* = 8.6 Hz, 4H), 7.23 (d, *J* = 8.9 Hz, 4H), 7.16 (ddd, *J* = 8.5, 6.8, 1.6 Hz, 4H), 5.82 (s, 4H), 1.71 (s, 12H), 1.56 (s, 12H) ppm. ¹³C NMR (CDCl₃, 75 MHz) δ 157.2 (C), 154.6 (C), 142.4 (C), 140.6 (C), 136.8 (C), 133.9 (C), 132.4 (C), 130.1 (CH), 130.0 (C), 129.4 (CH), 128.0 (CH), 127.3 (CH), 125.4 (CH), 123.9 (CH), 123.5 (CH), 122.8 (CH), 121.5 (C), 16.5 (CH₃), 16.3 (CH₃) ppm. FTIR *ν* 1547, 1507, 1467, 1294, 1155, 981 cm⁻¹.

6b: 61 mg (50%). Orange solid. *R*_f = 0.10 (hexane/CH₂Cl₂ 1:1). ¹H NMR (CDCl₃, 300 MHz) δ 8.15 (s, 4H), 7.76 (d, *J* = 8.1 Hz, 4H), 7.63 (s, 4H), 7.33 (dd, *J* = 8.1, 6.7 Hz, 4H), 7.15 (dd, *J* = 8.6, 6.8 Hz, 4H), 7.10 (d, *J* = 8.6 Hz, 4H), 5.86 (s, 4H), 1.70 (s, 12H), 1.58 (s, 12H) ppm. ¹³C NMR (CDCl₃, 75 MHz) δ 156.8 (C), 150.8 (C), 142.7 (C), 140.4 (C), 136.9 (C), 133.2 (C), 133.0 (C), 132.1 (CH), 130.2 (C), 130.0 (CH), 127.2 (CH), 127.1 (CH), 125.8 (CH), 124.5 (CH), 122.9 (CH), 122.7 (C), 119.3 (C), 16.5 (CH₃), 15.7 (CH₃) ppm. FTIR *ν* 1550, 1508, 1492, 1394, 1294, 1178, 1158, 1045, 983 cm⁻¹.

4.2. Photophysical Properties

The absorption spectra were recorded by UV-Vis-NIR Spectroscopy (model Cary 7000, Agilent Technologies, Madrid, Spain) equipped with two lamps (halogen lamp for Vis-IR region and deuterium lamp for UV region).

The fluorescence measurements were recorded with an Edinburgh Instruments Spectrofluorometer (FLSP920 model, Livingston, UK) equipped with a xenon flash lamp 450 W as the excitation source. The fluorescence spectra were corrected from the wavelength dependence on the detector sensibility. The fluorescence quantum yields of the photosensitizers were measured using the relative method, using as a standard sample pyromethene 567 ($\phi_{fl} = 0.85$ in acetone).

Radiative decay curves were recorded in the same Edinburgh Instrument by Time-Correlated Single-Photon Counting Technique (TC-SPC), using a microchannel plate detector (Hamamatsu C4878) with picosecond time resolution (≈ 100 ps). Fluorescence decay curves were monitored at the maximum emission wavelength after excitation using a fianium super-continuous wavelength tunable laser with 150 ps FWHM pulses.

The singlet oxygen quantum yield (ϕ_{Δ}) was determined using a direct method measuring its phosphorescence at 1276 nm employing a NIR detector (InGaAs detector, Hamamatsu G8605-23), integrated into the same Edinburgh spectrofluorometer upon continuous monochromatic excitation (450 W Xenon lamp) of the sample in cells of 1 cm in front configuration (front face), 40° and 50° to the excitation and emission beams, respectively, and angled 30° to the plane formed by the direction of incidence. The value was obtained using the average from at least five different concentrations (ranging from 2×10^{-6} M to 5×10^{-5} M) and using a commercial photosensitizer as the reference: 8-methylthio-2,6-diiodoBODIPY (MeSBDP, CAS-1835282-63-7, $\phi_{\Delta} = 0.91$ in CHCl₃, [19]).

Author Contributions: Conceptualization, V.M.-M. and S.d.l.M.; investigation, S.S.-B., J.J., R.P.-M., B.L.M. and F.M.; writing—original draft preparation, S.S.-B. and R.P.-M., with input from all the authors; writing—review and editing, B.L.M., V.M.-M. and S.d.l.M.; supervision, S.d.l.M.; funding acquisition, V.M.-M. and S.d.l.M. All authors have read and agreed to the published version of the manuscript.

Funding: This research was funded by MICINN (PID2020-114755GB-C32 and PID2020-114347RB-C32) and the Basque Government (IT1639-22). S.S.-B. and R.P.-M., respectively, thank CM/UCM and MICINN (MARSA21/71) for research contracts.

Institutional Review Board Statement: Not applicable.

Informed Consent Statement: Not applicable.

Data Availability Statement: Not applicable.

Conflicts of Interest: The authors declare no conflict of interest. The funders had no role in the design of the study; in the collection, analyses, or interpretation of data; in the writing of the manuscript; or in the decision to publish the results.

References

1. Zhao, J.; Wu, W.; Sun, J.; Guo, S. Triplet Photosensitizers: From Molecular Design to Applications. *Chem. Soc. Rev.* **2013**, *42*, 5323–5351. [[CrossRef](#)] [[PubMed](#)]
2. Zhao, X.; Hou, Y.; Liu, L.; Zhao, J. Triplet Photosensitizers Showing Strong Absorption of Visible Light and Long-Lived Triplet Excited States and Application in Photocatalysis: A Mini Review. *Energy Fuels* **2021**, *35*, 18942–18956. [[CrossRef](#)]
3. Pang, E.; Zhao, S.; Wang, B.; Niu, G.; Song, X.; Lan, M. Strategies to Construct Efficient Singlet Oxygen-Generating Photosensitizers. *Coord. Chem. Rev.* **2022**, *472*, 214780. [[CrossRef](#)]
4. Mahammed, A.; Gross, Z. Corroles as Triplet Photosensitizers. *Coord. Chem. Rev.* **2019**, *379*, 121–132. [[CrossRef](#)]
5. Schäferling, M. The Art of Fluorescence Imaging with Chemical Sensors. *Angew. Chem. Int. Ed.* **2012**, *51*, 3532–3554. [[CrossRef](#)] [[PubMed](#)]
6. Boens, N.; Verbelen, B.; Ortiz, M.J.; Jiao, L.; Dehaen, W. Synthesis of BODIPY Dyes through Postfunctionalization of the Boron Dipyrromethene Core. *Coord. Chem. Rev.* **2019**, *399*, 213024. [[CrossRef](#)]
7. Bañuelos, J. BODIPY Dye, the Most Versatile Fluorophore Ever? *Chem. Rec.* **2016**, *16*, 335–348. [[CrossRef](#)] [[PubMed](#)]
8. Chen, K.; Dong, Y.; Zhao, X.; Imran, M.; Tang, G.; Zhao, J.; Liu, Q. Bodipy Derivatives as Triplet Photosensitizers and the Related Intersystem Crossing Mechanisms. *Front. Chem.* **2019**, *7*, 821. [[CrossRef](#)]
9. Bassan, E.; Gualandi, A.; Cozzi, P.G.; Ceroni, P. Design of BODIPY Dyes as Triplet Photosensitizers: Electronic Properties Tailored for Solar Energy Conversion, Photoredox Catalysis and Photodynamic Therapy. *Chem. Sci.* **2021**, *12*, 6607–6628. [[CrossRef](#)] [[PubMed](#)]
10. Kamkaew, A.; Lim, S.H.; Lee, H.B.; Kiew, L.V.; Chung, L.Y.; Burgess, K. BODIPY Dyes in Photodynamic Therapy. *Chem. Soc. Rev.* **2012**, *42*, 77–88. [[CrossRef](#)] [[PubMed](#)]
11. Hu, W.; Zhang, R.; Zhang, X.-F.; Liu, J.; Luo, L. Halogenated BODIPY Photosensitizers: Photophysical Processes for Generation of Excited Triplet State, Excited Singlet State and Singlet Oxygen. *Spectrochim. Acta A Mol. Biomol. Spectrosc.* **2022**, *272*, 120965. [[CrossRef](#)] [[PubMed](#)]
12. Cakmak, Y.; Kolemen, S.; Duman, S.; Dede, Y.; Dolen, Y.; Kilic, B.; Kostereli, Z.; Yildirim, L.T.; Dogan, A.L.; Guc, D.; et al. Designing Excited States: Theory-Guided Access to Efficient Photosensitizers for Photodynamic Action. *Angew. Chem. Int. Ed.* **2011**, *50*, 11937–11941. [[CrossRef](#)] [[PubMed](#)]
13. Zou, J.; Yin, Z.; Ding, K.; Tang, Q.; Li, J.; Si, W.; Shao, J.; Zhang, Q.; Huang, W.; Dong, X. BODIPY Derivatives for Photodynamic Therapy: Influence of Configuration versus Heavy Atom Effect. *ACS Appl. Mater. Interfaces* **2017**, *9*, 32475–32481. [[CrossRef](#)] [[PubMed](#)]
14. Wang, D.-G.; Zhang, L.-N.; Li, Q.; Yang, Y.; Wu, Y.; Fan, X.; Song, M.; Kuang, G.-C. Dimeric BODIPYs with Different Linkages: A Systematic Investigation on Structure-Properties Relationship. *Tetrahedron* **2017**, *73*, 6894–6900. [[CrossRef](#)]
15. Gartzia-Rivero, L.; Sánchez-Carnerero, E.M.; Jiménez, J.; Bañuelos, J.; Moreno, F.; Maroto, B.L.; López-Arbeloa, I.; de la Moya, S. Modulation of ICT Probability in Bi(Polyarene)-Based O-BODIPYs: Towards the Development of Low-Cost Bright Arene-BODIPY Dyads. *Dalton Trans.* **2017**, *46*, 11830–11839. [[CrossRef](#)] [[PubMed](#)]
16. Jiménez, J.; Prieto-Montero, R.; Maroto, B.L.; Moreno, F.; Ortiz, M.J.; Oliden-Sánchez, A.; López-Arbeloa, I.; Martínez-Martínez, V.; de la Moya, S. Manipulating Charge-Transfer States in BODIPYs: A Model Strategy to Rapidly Develop Photodynamic Theragnostic Agents. *Chem. Eur. J.* **2020**, *26*, 601–605. [[CrossRef](#)] [[PubMed](#)]
17. Jiménez, J.; Prieto-Montero, R.; Serrano, S.; Stachelek, P.; Rebollar, E.; Maroto, B.L.; Moreno, F.; Martínez-Martínez, V.; Pal, R.; García-Moreno, I.; et al. BINOL blocks as accessible triplet state modulators in BODIPY dyes. *Chem. Commun.* **2022**, *58*, 6385–6388. [[CrossRef](#)] [[PubMed](#)]

18. Li, T.; Gu, W.; Yu, C.; Lv, X.; Wang, H.; Hao, E.; Jiao, L. Syntheses and Photophysical Properties of meso-Phenylene ridged Boron Dipyrromethene Monomers, Dimers and Trimer. *Chin. J. Chem.* **2016**, *34*, 989–996. [[CrossRef](#)]
19. Prieto-Montero, R.; Sola-Llano, R.; Montero, R.; Longarte, A.; Arbeloa, T.; López-Arbeloa, I.; Martínez-Martínez, V.; Lacombe, S. Methylthio BODIPY as a standard triplet photosensitizer for singlet oxygen production: A photophysical study. *Phys. Chem. Chem. Phys.* **2019**, *21*, 20403–20414. [[CrossRef](#)] [[PubMed](#)]